Journal of Applied Mechanics, Mechatronics and Energy System,
Vol. xx, Issue xx
October 2026
ISSN: XXXX-YYYY

Numerical Investigation of Twin Savonius Rotor Configuration for Tidal Current Energy Conversion

Alifia Laila Rizki[1], Sony Junianto[2*], Teguh Hady Ariwibowo[3]

[1,2,3]*Department of Mechanical and Energy Engineering, Politeknik Elektronika Negeri Surabaya, Jl. Raya ITS, Sukolilo, Surabaya 60111, Indonesia*

**Corresponding author: Sony Junianto; email: sony@pens.ac.id*

Manuscript received July 23, 2026, revised September 3, 2026, accepted October 26, 2026
DOI: zz.yyyyy/xxxxx.pp134-1199

Abstract – *Indonesia is committed to achieving Net Zero Emissions by accelerating the transition toward renewable energy, including tidal current energy, which has substantial potential in the Toyapekah Strait. This study numerically investigates the performance of a twin Savonius Vertical Axis Tidal Current Turbine (VATCT) arranged in a side-by-side Canard layout and combined with NACA 63(4)221 flow disturbances. Two disturbance distances, 0.7D and 1D, are compared with a baseline configuration using two-dimensional transient Computational Fluid Dynamics (CFD) with the SST k-ω turbulence model. Turbine performance is evaluated using torque and power coefficients over several Tip Speed Ratios (TSRs) and inlet velocities. At 1.419 m/s, the baseline configuration produces a higher Cp than the disturbed cases, whereas at 3.37 m/s the 1D configuration reaches the maximum Cp of 0.4685 at TSR 0.8. The results therefore show that the influence of the flow disturbance is dependent on inlet velocity and TSR rather than universally beneficial. Flow and pressure contours at the maximum-Cp condition indicate stronger flow redirection toward the advancing blade and modification of the wake around the returning blade.*

Keywords: *Computational Fluid Dynamics (CFD), Flow Disturbance, Savonius Turbine, Tidal Current, Vertical Axis Turbine*

I. Introduction

PLN's installed electricity capacity and number of power generation units total 45,095.19 MW and 6,446 units, with 31,202.08 MW (65.29%) located in Java [1]. Indonesia's commitment to Net Zero Emissions (NZE) by 2060 involves phasing out coal-fired power plants, marked by the cessation of new coal-fired power plant construction [2]. In line with this, the target for the share of renewable energy is set at 65.5 GW [3]. The relevant ministry estimates that renewable energy capacity can be expanded to 3,686 GW [4]. Covering nearly 70% of the Earth's surface, the ocean provides enormous renewable energy potential, with tidal current energy emerging as a reliable and sustainable resource. Therefore, tidal current turbines are regarded as a promising technology for future global energy generation.

Indonesia and renewable tidal energy will always go hand in hand [5]. This is because Indonesia’s tidal energy potential features tidal currents with speeds of less than 1.5 m/s [6]. The Toyapekah Strait, located on Nusa Penida Island, has tidal currents with a more widespread distribution of current directions. It features strong current speeds ranging from 0.5 m/s to 3.2 m/s, with currents lasting approximately 12 to 22 hours per day [7], [8]. Accurate tidal current characterization is essential for optimizing turbine deployment and performance [9].

Tidal current energy can be converted using Vertical Axis Tidal Current Turbines (VATCTs) or Horizontal Axis Tidal Current Turbines (HATCTs) [5], [10]. Among vertical-axis concepts, Savonius rotors are drag-based and are attractive for low-current-speed operation because of their simple geometry and self-starting characteristics [11].

Previous studies have improved Savonius turbine performance using flow-control devices and geometric modification. Circular-cylinder disturbances placed near the advancing blade have been reported to improve Cp for selected diameter ratios and TSRs [12]. Airfoil-shaped

deflectors have also been investigated to improve Savonius performance [13], while rear deflectors can reduce adverse loading on the returning blade [16]. Other studies have examined blade arc angle, blade number, and operating TSR [14], [17], [18]. These studies demonstrate that the effect of a disturbance depends strongly on its geometry, position, and operating condition.

However, most previous flow-disturbance studies have focused on a single Savonius rotor, whereas studies of twin-rotor systems have primarily emphasized rotor arrangement and spacing. The combined hydrodynamic interaction of a side-by-side twin Savonius system with airfoil-shaped disturbances positioned upstream and in the inter-turbine wake has not been systematically evaluated over different inlet velocities and TSRs. To address this gap, the present study investigates a twin Savonius turbine in a Canard layout with a fixed inter-turbine spacing of 1.5D and compares three configurations: baseline, 0.7D flow disturbance, and 1D flow disturbance. This configuration differs from earlier single-rotor disturbance studies by explicitly considering the coupled wake interaction between two co-rotating Savonius rotors.

II. Methodology

A. Turbine Configurations and Variations

The Savonius turbine profile in this study utilizes a three-bladed configuration, following the optimized designs established in [12], [14], [16], [17], [20]. Based on calculations from Equations (1) and (2), the turbine diameter is determined to be 3.09 m. A blade arc angle of 120° is implemented to achieve higher torque accumulation, as suggested by [16], as shown in Fig. 1.

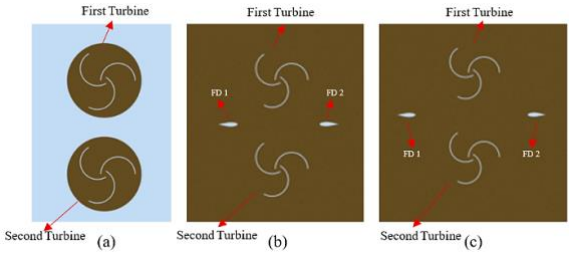


Fig. 1. Geometry configurations: (a) twin Savonius turbine without flow disturbance, (b) with 0.7D flow disturbance, (c) with 1D flow disturbance

Performance analysis is conducted via 2D numerical simulations using Computational Fluid Dynamics (CFD). The specific turbine power and swept area calculations are detailed below:

$$P = 1/2 \times \rho \times A \times V^3 \quad (1)$$

$$A = D \times H \quad (2)$$

where P is the theoretical fluid power, ρ is fluid density, A is swept area, V is inlet velocity, D is rotor diameter, and H is blade height.

The torque coefficient (Ct) and power coefficient (Cp) used to quantify turbine performance, along with the Tip Speed Ratio (λ or TSR), are defined as follows:

$$C_t = T / (0.5 \rho A V^2 R) \quad (3)$$

$$C_p = T\omega / (0.5 \rho A V^3) = C_t \lambda \quad (4)$$

$$\lambda = \omega R / V \quad (5)$$

where T is turbine torque, R is rotor radius, ω is angular velocity, and λ is the Tip Speed Ratio (TSR).

The theoretical fluid power (P) available from tidal currents is estimated using Equation (1), which incorporates fluid density ρ, turbine swept area (A), and inlet velocity (V). The swept area is further defined in Equation (2) as the product of the rotor diameter (D) and blade height (H). The research geometry variations are listed in Table I.

TABLE I
RESEARCH GEOMETRY AND OPERATING PARAMETERS

Parameter	Dimension / Specification
Number of blades	3
Turbine Diameter (D)	3.09 m
Blade Arc Angle	120°
Flow disturbance Type	NACA 63(4)221
Overlap Ratio	0.1
Velocity variations	0.022; 1.419; 3.37 m/s
FD distance variations	0.7D; 1D
Turbine spacing	1.5D
TSR	0.2; 0.5; 0.8; 1.1

Expanding on the methodology in [14], this study utilizes an airfoil-shaped flow disturbance. Specifically, the NACA 63(4)221 profile was selected due to its ability to provide stable lift enhancement across various angles of attack and its effectiveness in maintaining flow attachment during specific operating conditions [21].

Building on previous research, this study adopts a side-by-side "Canard layout" for the twin-turbine configuration as proposed in [18]. A novel aspect of this work involves utilizing a specific inter-turbine spacing of 1.5D. To enhance performance, NACA 63(4)221 airfoil-shaped flow disturbances are positioned both upstream of the system and in the wake between the first and second turbines, a placement strategy derived from [14], as shown in Fig. 2.

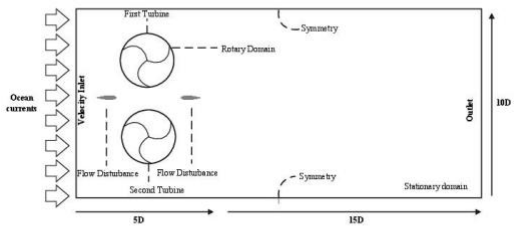


Fig. 2. Computational domain for 2D tidal current turbine simulation

The computational domain is sized at 10D × 20D based on established studies [14]. Unidirectional rotation was

used in this study for both turbines. Using a 2D solver, the simulation calculates turbine torque across the defined rotational velocity range.

B. Meshing

To ensure numerical accuracy, the computational domain is discretized using a hybrid mesh strategy. An unstructured triangular mesh is applied in the rotary domain to handle geometric complexity, while a structured mesh is used in the stationary domain for computational efficiency. Finer mesh refinement is applied near the turbine blades to accurately capture flow details and gradients. Fig. 3 and Table II present the mesh details and quality metrics.

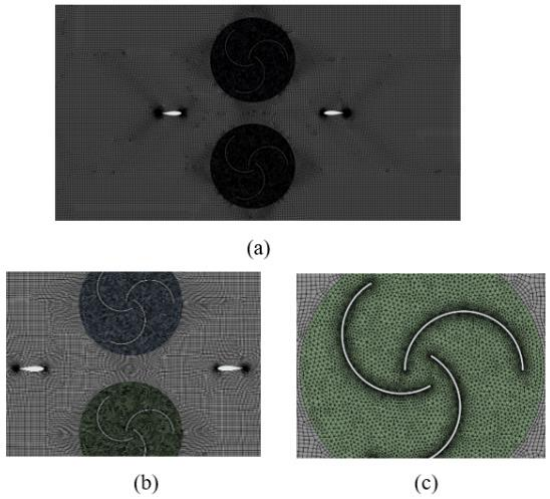


Fig. 3. Mesh for the 1D flow-disturbance configuration: (a) complete domain, (b) rotary domain, (c) near-blade refinement

TABLE II
MESH QUALITY PARAMETERS

Mesh Parameter	Value
Skewness	0.5796
Element quality	0.47439
Orthogonal quality	0.5111
Aspect ratio	3.4201

C. CFD Setup

Following the meshing process, CFD configurations are established, including the selection of physical models, boundary conditions, and relevant numerical parameters. Transient simulations are conducted to capture the dynamic flow behavior caused by turbine rotation. The k-ω SST turbulence model is applied to accurately predict near-wall flow characteristics, with fresh water as the working fluid. Boundary conditions include the inlet velocity, turbine wall, and rotational speed. The sliding mesh method is used to represent blade rotation and the interaction between moving and stationary domains, while the rotational velocity, number of time steps, and time step size are determined using Equations (6)–(8) based on previous studies [22]:

$$\omega = (TSR \times V) / R \quad (6)$$

$$NTS = N \times (360 / \theta) \quad (7)$$

$$TSS = N / (\omega \times 0.15915 \times NTS) \quad (8)$$

The rotational velocity (ω) of the Savonius turbine is calculated using Equation (6), which relates the Tip Speed Ratio (TSR), inlet velocity (V), and rotor radius (R) to represent the intended operating condition accurately. The transient simulation setup is defined through the Number of Time Steps (NTS) and the Time Step Size (TSS). Equation (7) determines the NTS based on the angular displacement, while Equation (8) calculates the TSS to ensure convergence and accurate capture of unsteady flow behavior during turbine rotation.

The simulation uses a pressure-based transient solver with the k-ω SST turbulence model to predict flow separation and near-wall effects effectively. The PISO algorithm is applied for pressure–velocity coupling, while higher-order discretization schemes are used to minimize numerical diffusion and improve solution accuracy.

III. Result

A. Verification

The verification of numerical results is conducted following the completion of the CFD setup in Fluent and the execution of the simulation process. This stage is essential to ensure that the selected physical models and numerical methods accurately represent real-world flow phenomena. Verification is performed by comparing the current simulation results against established experimental data to determine the reliability and validity of the numerical output before proceeding to the primary analysis.

In this process, the primary parameters utilized for comparison are the relationship between the Coefficient of Power (Cp) and the Tip Speed Ratio (TSR) alongside the torque values across varying flow velocities. These parameters are selected for their ability to provide a comprehensive representation of turbine performance, allowing for a rigorous evaluation of the alignment between numerical simulations and experimental benchmarks, particularly regarding velocity variations, as presented in Table III.

TABLE III
COMPARISON OF NUMERICAL SIMULATION AND EXPERIMENTAL CP

Velocity (m/s)	TSR	Cp Experiment	Cp Simulation Numeric	Error (%)
0.5	0.4	0.247	0.2443	0.7%
0.5	1.0	0.258	0.2787	7.0%
0.5	1.4	0.272	0.2404	11.0%

Both datasets show a similar increasing trend in the Coefficient of Power (Cp) with increasing Tip Speed Ratio (TSR). At TSR 0.4, the numerical Cp value is slightly lower than the experimental result, while at TSR

1.0 both methods produce nearly identical values, indicating good agreement between the simulation and experimental data.

At TSR 1.4, the numerical results increase more significantly, resulting in a larger deviation from the experimental data. These differences may be caused by simplifications in the numerical model and limitations in the experimental setup. However, the overall trends remain consistent and within an acceptable error range, confirming the validity of the numerical approach for further analysis.

B. Effect of Tip Speed Ratio on Turbine Performance

This study evaluates turbine performance at a flow velocity of 1.419 m/s, chosen as a stable operating condition for tidal currents. The analysis examines the relationship between the Tip Speed Ratio (TSR) and the Coefficient of Power (Cp) at different rotational speeds. Three configurations are compared: without FD, with 0.7D FD, and with 1D FD. The objective is to identify the optimum operating condition and evaluate the effect of the flow disturbance on turbine performance using Cp versus TSR curves, as shown in Fig. 4.

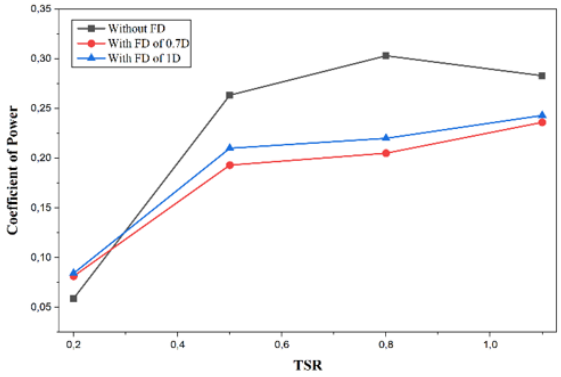


Fig. 4. Variation of Power Coefficient (Cp) with Tip Speed Ratio (TSR) at a flow velocity of 1.419 m/s

The performance analysis is conducted at a flow velocity of 1.419 m/s because this condition provides stable and reliable turbine operation. At this velocity, the relationship between TSR and Cp can be clearly observed, where the performance increases from TSR 0.2 to 0.8 before slightly decreasing, indicating the optimum operating condition has been reached. This result shows that introducing a flow disturbance does not automatically improve performance at every operating condition.

The lower Cp of the 0.7D and 1D cases at 1.419 m/s suggests that the additional blockage and flow redirection can introduce losses that are not compensated by an increase in positive blade torque. In contrast, at 3.37 m/s the 1D configuration produces the highest Cp (0.4685 at TSR 0.8). The change in ranking with inlet velocity indicates that the benefit of the disturbance is momentum-dependent: at higher velocity, the redirected jet and pressure difference acting on the advancing blade can become sufficiently strong to offset disturbance-induced losses, whereas at lower velocity the same device may primarily increase resistance and wake interference.

C. In-Depth Analysis of Flow and Pressure Characteristics

The performance of the twin Savonius turbine is influenced by both the Tip Speed Ratio (TSR) and the incoming flow velocity. Although the analysis at 1.419 m/s provides a stable comparison, the highest power coefficient (Cp) is achieved at a higher flow velocity of 3.37 m/s, particularly at TSR 0.8, indicating the turbine's optimum operating condition. To further analyze the flow behavior at this optimum condition, velocity contour analysis is conducted at TSR 0.8 and a flow velocity of 3.37 m/s, as shown in Fig. 5 and Fig. 6.

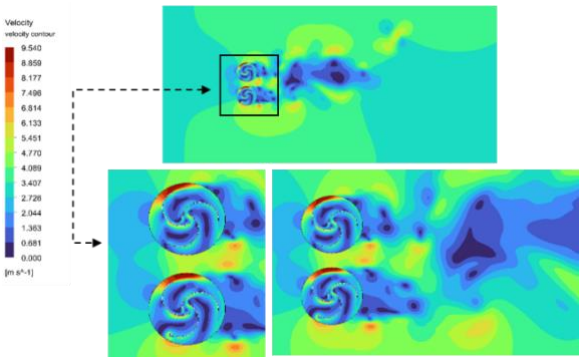


Fig. 5. Velocity contour at V = 3.37 m/s, TSR = 0.8, without flow disturbance

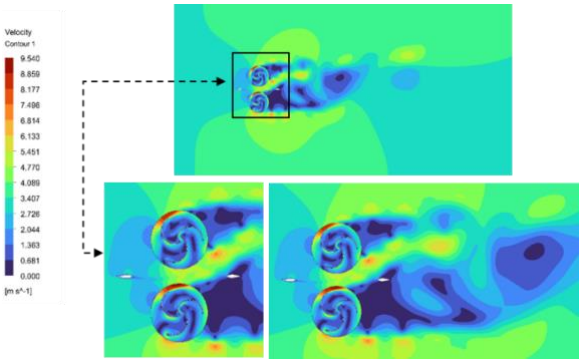


Fig. 6. Velocity contour at V = 3.37 m/s, TSR = 0.8, with 1D flow disturbance

This phenomenon indicates that flow disturbances at a 1D distance can modify the flow before it enters the rotor. This distance provides sufficient space for the flow to adjust its direction, so that the flow reaching the advancing blade has greater momentum. At the same time, the presence of flow disturbances also reduces the intensity of the flow interacting with the returning blade, thereby reducing the drag that causes negative torque. This configuration effectively accelerates and directs high-velocity flow toward the advancing blades while shielding the returning blades, thereby reducing negative torque and improving energy conversion efficiency.

In the analysis results presented here, the obtained torque values yield a Cp value that meets existing theoretical standards. These flow characteristics align with

the results of the torque and power coefficient analyses, which show that the 1D flow disturbance configuration yields the best performance with a maximum Cp value of 0.4685 at a TSR of 0.8.

The pressure contour comparison at TSR 0.8 and a flow velocity of 3.37 m/s is presented in Fig. 7 and Fig. 8.

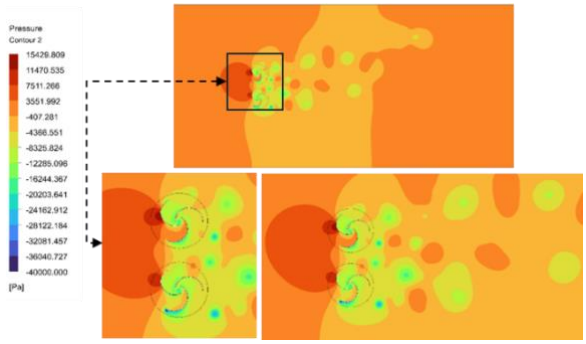


Fig. 7. Pressure contour at V = 3.37 m/s, TSR = 0.8, without flow disturbance

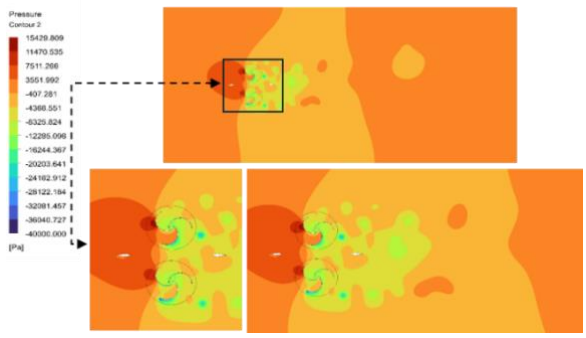


Fig. 8. Pressure contour at V = 3.37 m/s, TSR = 0.8, with 1D flow disturbance

Fig. 7 and Fig. 8 compare the pressure contours of the baseline configuration and the 1D flow disturbance configuration. In the baseline case, pressure distribution is governed solely by the direct interaction between the incoming flow and the rotor blades. A high-pressure region develops on the concave surface of the advancing blade due to flow stagnation, generating the primary driving torque. Meanwhile, the convex surface of the returning blade experiences a broad low-pressure region, which increases negative torque and reduces the overall turbine performance [23], [24], [25].

With the 1D disturbance, the upstream pressure and velocity fields are redistributed before reaching the rotor. The high-pressure region on the advancing-blade side is maintained while the wake and low-pressure region near the returning blade are modified. Together with the velocity contours, this indicates that the disturbance alters the loading distribution at the maximum-Cp operating point. Quantification of the corresponding negative-torque reduction should be based on torque-versus-angle data rather than on contour interpretation alone.

Following the general performance analysis, a more detailed investigation is required to understand the fundamental mechanisms governing turbine behavior. While the previous sections provide a comparative evaluation across different TSR values and flow velocities, they do not fully explain the physical reasons behind the observed performance variations.

Therefore, a specific operating condition is selected for in-depth analysis, namely TSR 0.8 with a flow velocity of 3.37 m/s using a 1D flow disturbance. This configuration corresponds to the highest power coefficient obtained in this study, indicating the most efficient energy conversion process. The selection of this condition is not only based on its superior performance but also on its ability to represent the optimal interaction between rotational speed, flow momentum, and geometric modification. At this point, the balance between incoming flow energy and blade motion produces the most effective drag force and torque generation. In conclusion, tidal current turbine performance is significantly influenced by the combination of flow velocity, TSR, and flow disturbance configuration. Consequently, real-world applications must carefully select turbine configurations based on site-specific flow characteristics to achieve maximum performance [26].

IV. Conclusion

This study numerically evaluates a twin Savonius tidal current turbine in a Canard layout with baseline, 0.7D, and 1D flow-disturbance configurations. The effect of the disturbance depends on inlet velocity and TSR. At V = 1.419 m/s, the baseline configuration produces a higher Cp than the disturbed configurations, indicating that the added flow-control device can introduce losses under some operating conditions. At V = 3.37 m/s and TSR = 0.8, however, the 1D configuration gives the highest Cp obtained in this study, 0.4685.

Velocity and pressure contours at the maximum-Cp condition show that the 1D disturbance redirects the incoming flow toward the advancing-blade region and modifies the wake around the returning blade. These observations are consistent with improved rotor loading at this specific operating point, but a quantitative claim of negative-torque reduction must be confirmed using torque-versus-rotor-angle data. Overall, the results do not support the conclusion that the 1D configuration always improves performance; instead, the preferred configuration should be selected according to the local flow velocity and turbine TSR. Further three-dimensional CFD and experimental validation are recommended.

ACKNOWLEDGEMENTS

The authors would like to thank the Fluid Laboratory and the Electromagnetic Energy Conversion Laboratory at Politeknik Elektronika Negeri Surabaya for providing the facilities needed to conduct this research.

REFERENCES

[1] Statistik Ketenagalistrikan 2023, PT PLN (Persero), Jakarta, Indonesia, 2024.

[2] Kementerian ESDM RI, "Strategi Penurunan Emisi Sektor Ketenagalistrikan Menuju Net Zero Emission 2060," Siaran Pers Kementerian Energi dan Sumber Daya Mineral, 2025.

[3] Direktorat Jenderal EBTKE, "Akselerasi Transisi Energi Baru Terbarukan Nasional," Kementerian ESDM RI, Jakarta, 2025.

[4] Kementerian ESDM RI, "Potensi dan Roadmap Pengembangan Energi Baru Terbarukan Indonesia," Publikasi Ditjen Ketenagalistrikan, 2025.

[5] Rasgianti et al., "Learning from field testing experiences for developing small scale tidal current energy conversion system," IOP Conf. Series: Earth and Environmental Science, vol. 1265, no. 1, art. no. 012016, 2023. https://doi.org/10.1088/1755-1315/1265/1/012016

[6] Kementerian ESDM RI, "Road Map Penelitian dan Pengembangan Energi Arus Laut Nasional," Balitbang ESDM, 2025.

[7] C. L. Dewangi, D. N. Sugianto, A. Rifai, and A. Yuningsih, "Kajian potensi energi arus laut di Selat Toyapakeh, Nusa Penida, Bali," Jurnal Oseanografi, vol. 6, no. 1, pp. 22–29, 2017.

[8] B. Rachmat and D. Ilahude, "Estimation of sea current energy potential by using calculation models of horizontal axis current turbine in Toyapakeh Strait, Nusa Penida, Bali," Bulletin of the Marine Geology, vol. 32, no. 2, pp. 51–60, 2017.

[9] S. Junianto et al., "Experience in oceanographic surveys for designing 100 kW tidal current energy conversion systems," International Journal of Offshore and Coastal Engineering, vol. 7, no. 1, pp. 50–55, 2023.

[10] O. B. Yaakob, D. T. Suprayogi, M. P. Abdul Ghani, and K. B. Tawi, "Experimental studies on Savonius-type vertical axis turbine for low marine current velocity," International Journal of Engineering, Transactions A: Basics, vol. 26, no. 1, pp. 91–98, 2013. https://doi.org/10.5829/idosi.ije.2013.26.01a.12

[11] S. Junianto, W. N. Fadilah, A. F. Adila, Tuswan, D. Satrio, and S. Musabikha, "State of the art in floating tidal current power plant using multi-vertical-axis-turbines," in Proc. 2022 International Electronics Symposium (IES), pp. 97–103, 2022. https://doi.org/10.1109/IES55876.2022.9888749

[12] D. Satrio and S. Junianto, "Numerical study of a circular cylinder effect on the vertical axis Savonius water turbine performance at the side of the advancing blade with horizontal distance variations," Ocean Engineering, vol. 248, art. no. 110820, 2022.

[13] K. Layeghmand, N. Ghiasi Tabari, and M. Zarkesh, "Improving efficiency of Savonius wind turbine by means of an airfoil-shaped deflector," Journal of the Brazilian Society of Mechanical Sciences and Engineering, vol. 42, no. 10, art. no. 528, 2020. https://doi.org/10.1007/s40430-020-02598-7

[14] D. Satrio, Suntoyo, and S. Musabikha, "Validation study for Savonius vertical axis marine current turbine using CFD simulation," International Journal of Marine Energy, vol. 20, pp. 112–122, 2017.

[15] D. Satrio, Suntoyo, and I. K. A. P. Utama, "The advantage of flow disturbance for vertical-axis turbine in low current velocity," Sustainable Energy Technologies and Assessments, vol. 49, art. no. 101740, 2022.

[16] F. Guo, B. Song, Z. Mao, and W. Tian, "Experimental and numerical validation of the influence on Savonius turbine caused by rear deflector," Energy, vol. 196, art. no. 117132, 2020. https://doi.org/10.1016/j.energy.2020.117132

[17] A. Sakti, A. Prasetyo, D. D. D. P. Tjahjana, and S. Hadi, "The horizontal axis type of Savonius water turbine in pipe using SolidWorks simulation," AIP Conf. Proc., vol. 2097, no. 1, art. no. 030012, 2019. https://doi.org/10.1063/1.5098217

[18] S. Junianto, R. W. Prastianto, and Mukhtasor, "An analytical approach to modeling of motion-response of floating structure for ocean renewable energy conversion system," Applied Mechanics and Materials, vol. 874, pp. 44–49, 2018. https://doi.org/10.4028/www.scientific.net/AMM.874.44

[19] A. A. Akbar Firmansyah, S. Junianto, and J. Pratilastiarso, "Numerical analysis of Savonius ocean current turbine performance in Kepa Strait," in Proc. 2025 International Electronics Symposium (IES), pp. 58–64, 2025. https://doi.org/10.1109/IES67184.2025.11161815

[20] D. Satrio and I. K. A. P. Utama, "Experimental investigation into the improvement of self-starting capability of vertical-axis tidal current turbine," Energy Reports, vol. 7, pp. 4587–4594, 2021. https://doi.org/10.1016/j.egyr.2021.07.027

[21] P. K. Nigam, N. Tenguria, and M. K. Pradhan, "Analysis of horizontal axis wind turbine blade using CFD," International Journal of Engineering, Science and Technology, vol. 9, no. 2, pp. 46–60, 2017. https://doi.org/10.4314/ijest.v9i2.5

[22] D. Satrio, I. K. A. P. Utama, and Mukhtasor, "The influence of time step setting on the CFD simulation result of vertical axis tidal current turbine," Journal of Mechanical Engineering and Sciences, vol. 12, no. 3, pp. 3399–3409, 2018.

[23] D. Satrio, F. Y. Muhammad, Mukhtasor, S. Rahmawati, S. Junianto, and S. Musabikha, "Numerical simulation of cross-flow Savonius turbine for locations with low current velocity in Indonesia," Journal of the Brazilian Society of Mechanical Sciences and Engineering, vol. 44, no. 8, art. no. 362, 2022. https://doi.org/10.1007/s40430-022-03620-w

[24] S. R. Kaswarie, S. Junianto, and J. Pratilastiarso, "Circular flow disturbance effect to Darrieus tidal current turbine performance in Kepa Strait," in Proc. 2025 International Electronics Symposium (IES), pp. 108–114, 2025. https://doi.org/10.1109/IES67184.2025.11161777

[25] S. Junianto, R. W. Prastianto, and Mukhtasor, "Studi numerik peningkatan kinerja pada turbin arus laut ganda berputar searah," ROTASI, vol. 25, no. 2, pp. 8–14, 2023. https://doi.org/10.14710/rotasi.25.2.1-7

[26] S. Junianto, "Studi interaksi struktur terapung dengan kinerja turbin sumbu vertikal ganda dari pembangkit listrik tenaga arus laut," Disertasi Doktor, Institut Teknologi Sepuluh Nopember, Surabaya, 2020.